

The MRC OX-62 Antigen: A Useful Marker in the Purification of Rat Veiled Cells with the Biochemical Properties of an Integrin

By M. Brenan and M. Puklavec

From the Medical Research Council Cellular Immunology Unit, Sir William Dunn School of Pathology, University of Oxford, Oxford OX1 3RE, England

Summary

A mouse immunoglobulin G1 monoclonal antibody (mAb), MRC OX-62 (OX-62), was raised against density gradient-enriched rat veiled (dendritic) cells obtained from lymph. In suspensions of lymphoid cells, the OX-62 mAb only labeled cells with the characteristics of veiled cells. The OX-62 mAb was used with a magnetic cell sorter to enrich or deplete veiled cells, and the enriched veiled cells were potent stimulators in the primary allogeneic mixed leukocyte reaction. Immunohistochemical staining of tissue sections showed that the OX-62 mAb did not label all classical dendritic cells and was not restricted to this cell type. In lymphoid tissues, the labeling correlated with dendritic cells, but in skin, major histocompatibility complex class II⁺ cells were OX-62⁻, while another CD3⁺ cell with dendritic morphology was strongly OX-62⁺. It seems that the OX-62 mAb may be restricted to dendritic cells and probably to γ/δ T cells. The OX-62 mAb will be of use in delineating minor subsets of cells with dendritic morphology in various tissues. Sodium dodecyl sulfate-polyacrylamide gel electrophoresis analysis of veiled cell-enriched populations immunoprecipitated with the OX-62 mAb gave bands with the biochemical characteristics of an integrin. The OX-62 mAb recognized the α -like subunit.

Dendritic cells are classified as a heterogeneous group of cells with dendritic morphology found in lymphoid and nonlymphoid tissues, and as veiled cells in lymph (1). Dendritic cells originate from bone marrow but the lineage is unresolved (2). Attention focused on dendritic cells after the isolation of the spleen dendritic cell and the observation that these cells are the most potent accessory cells identified at inducing primary T cell responses *in vitro* (3). The immunoregulatory role of dendritic cells *in vivo* is implicated by their presence in the T-dependent areas of secondary lymphoid organs (4, 5). Identification of dendritic cells is based on properties of the isolated spleen dendritic cell, which include dendritic morphology (6), constitutive expression of MHC class II (7), low phagocytic ability *in vitro* (8), and potent accessory function in the primary allogeneic MLR (3). The need for mAbs that are specific for dendritic cells is evident (9), but few useful mAbs are available (10–17), and anti-MHC class II mAbs are of limited value. One major problem in generating dendritic cell mAbs is that it is difficult to obtain large numbers of dendritic cells for immunization and there are no cell lines equivalent to normal dendritic cells (18–20). In this paper the production of a mouse IgG1 mAb (OX-62) useful for the purification of rat veiled cells and recognizing an antigen with the biochemical properties of an integrin is described.

Materials and Methods

Animals. BALB/c (H-2^d) and DBA/2 (H-2^k) inbred mice were obtained from the Sir William Dunn School of Pathology (Oxford). F₁ hybrids between these two strains were bred at the MRC Cellular Immunology Unit (Oxford). PVG (RT1^c) and AO (RT1^u) specific pathogen-free inbred rats were obtained from the MRC Cellular Immunology Unit. Rats were used at 8–12 wk, except where stated otherwise.

Mesenteric Lymphadenectomy. Cecal, mesenteric, postgastric, and portal lymph nodes were surgically removed using blunt dissection from 90-g male PVG rats. Mesenteric lymphadenectomized rats were allowed to recover for a minimum of 6 wk before thoracic duct cannulation.

Cell Populations. Cell suspensions were prepared in PBS containing 0.25% BSA. Thoracic duct leukocytes (TDL)¹ were obtained by thoracic duct cannulation of normal and mesenteric lymphadenectomized rats (21). Cells were collected overnight in ice-cold glucose saline (22) containing 20 U/ml heparin. Density gradient-enriched veiled cells were prepared from TDL obtained from mesenteric lymphadenectomized rats (MLNX TDL) by centrifugation over NycoprepTM 1.068 (Nycomed, Oslo, Norway). Thymocytes, splenocytes, and lymph node cells were obtained by removing appropriate organs and teasing into single cell suspen-

¹ Abbreviations used in this paper: MLNX TDL, thoracic duct leukocytes obtained from mesenteric lymphadenectomized rats; RAM, rabbit anti-mouse; TDL, thoracic duct leukocytes.

sions. PBL were prepared from blood obtained by cardiac puncture and separated over Isopaque-Ficoll. Bone marrow cells were obtained by flushing the marrow cavity of the femur with PBS. Resident peritoneal exudate cells were obtained from the peritoneal cavity of freshly killed rats. Elicited peritoneal exudate cells were obtained from the peritoneal cavity 4 d after intraperitoneal injection of 10 ml of thioglycollate broth. Con A blasts were obtained after a 3-d culture of lymph node cells at 10^6 /ml in RPMI 1640 supplemented with 5% heat-inactivated FCS, 2 mM glutamine, 1 mM sodium pyruvate, 2.5×10^{-5} M 2-ME, and antibiotics (supplemented RPMI), and 5 μ g/ml Con A. Con A blasts were separated over Isopaque-Ficoll and washed in α -methyl-D-mannoside (20 mg/ml). LPS blasts were obtained after a 2-d culture of lymph node cells at 10^6 /ml in supplemented RPMI and 10 μ g/ml LPS.

mAbs and Antibody Conjugates. The OX-62 hybridoma was produced by immunizing a BALB/c mouse with rat PVG density gradient-enriched veiled cells obtained from the cannulated thoracic duct of mesenteric lymphadenectomized rats. The immunization procedure was a combination of three intravenous and intraperitoneal injections with $5\text{--}10 \times 10^6$ cells at monthly intervals. 5 d after the last injection, the splenocytes were fused with NSO myeloma cells according to the method of Galfrè and Milstein (23). After growth of the hybrid cell lines, supernatants were screened for specificity by immunohistochemistry (see below). Selected hybridomas were cloned twice by limiting dilution. Ascites fluid was prepared in (BALB/c \times DBA/2)F₁ mice pretreated with pristane. The subclass of the OX-62 mAb was determined using an anti-mouse monoclonal isotyping kit (Serotec, Kidlington, Oxon, England).

Other mAbs used were SN3 (mouse anti-squid Sgp 1) (24), OX-6 (mouse anti-rat MHC class II, IgG1) (25), OX-8 (mouse anti-rat CD8, IgG1) (26), OX-12 (mouse anti-rat IgG κ chain, IgG2a) (27), OX-17 (mouse anti-rat MHC class II, IgG1) (28), OX-21 (mouse anti-human C3b inactivator, IgG1) (29), and OX-42 (mouse anti-rat CD18/CD11b, IgG2a) (30). mAbs were used as tissue culture supernatants, purified IgG from ascites fluid (31), and purified IgG from ascites fluid conjugated with biotin (32).

Other antibodies used were rabbit anti-mouse IgG mAb conjugated with peroxidase (RAM-peroxidase) (Dako, High Wycombe, Bucks, England), affinity-purified rabbit F(ab')₂ anti-mouse IgG mAb (Serotec) conjugated with fluorescein (RAM-FITC) (32), biotin (RAM-biotin) (32), and iodine (¹²⁵I-RAM) (33), and fluorescein-conjugated goat anti-mouse IgG1 (GAM-FITC) (Southern Biotechnology Associates, Inc., Birmingham, AL).

Flow Cytofluorography. Labeling of cells for analysis on a FACScan® (Becton Dickinson & Co., Mountain View, CA) was performed as described previously (32). Cells were gated on the scatter profiles to exclude dead cells and erythrocytes.

Magnetic Cell Sorting. The principle of the magnetic cell sorting system and conditions for labeling and sorting cells have been described in detail (34, 35). All incubations, washes, and sorting were carried out at 4°C in PBS containing 5 mM EDTA and 10 mM NaN₃. Briefly, 10⁹ cells were labeled in 5-ml mAb tissue culture supernatant for 30 min, washed, labeled in 1 ml RAM-biotin (10 μ g/ml) for 30 min, washed, labeled in 1 ml avidin-FITC (25 μ g/ml) (Becton Dickinson & Co., Cowley, Oxford, England) for 30 min, washed, and finally incubated in 1 ml containing 10 μ l biotinylated superparamagnetic microbeads (Becton Dickinson & Co.) for 5 min. Labeled cells were added to the appropriately sized column in the magnetic field. Unlabeled cells were collected in the first 10–15-ml volume. The column was washed to remove unlabeled, weakly bound, and dead cells. Magnetically labeled cells were eluted from the column outside the magnetic field. In some experiments en-

riched and depleted populations were further depleted of contaminating cells by a second magnetic sort. The efficiency of depletion and enrichment was determined by flow cytofluorography using a FACScan®.

MLR. 5×10^5 responder cells were cocultured with different numbers of irradiated (20 Gy) stimulator cells in supplemented RPMI in 96-well round-bottomed microtiter plates for 72 h at 37°C in a 5% CO₂ incubator. Samples were pulsed with 0.5 μ Ci [³H]TdR and incubated for a further 18 h. Samples were then harvested for incorporation of [³H]TdR. In some experiments OX-62 mAb and appropriate control mAbs were added as purified IgG at the start of culture.

Preparation of Specimens for Immunohistochemistry. For cryostat sections, organs were removed from rats, embedded in OCT (Miles, Elkhart, IN), and frozen in 2-methylbutane cooled in liquid nitrogen. 5- μ m cryostat sections were cut onto four-spot glass slides (C. A. Hendley, Essex, England), air dried, and stored desiccated at -70°C. For epidermal ear sheets, rat ears were split longitudinally and incubated in 116 mM NaCl, 2.6 mM KCl, 8 mM Na₂HPO₄, 1.4 mM KH₂PO₄, and 20 mM EDTA, pH 7.3, for 2 h at 37°C on a rotator (36). Epidermal sheets were separated using watchmaker's forceps under a dissecting microscope. For isolated cells, cytospin preparations were made using a cytocentrifuge, air dried, and stored desiccated at -70°C.

Immunohistochemistry. The peroxidase method was used for staining sections as described previously (37). All incubations were carried out at 4°C. Briefly, cryostat sections, epidermal sheets, and cytospin preparations were fixed in ethanol for 10 min, washed, incubated with mAb tissue culture supernatant for 60 min, except for epidermal ear sheets, which were incubated overnight, washed, incubated with RAM-peroxidase (25 μ g/ml) for 60 min, and washed. Peroxidase was visualized using 3,3'-diaminobenzidine tetrahydrochloride. Staining was enhanced using 0.01 M imidazole in the 3,3'-diaminobenzidine tetrahydrochloride solution. Slides were lightly counterstained with Harris' haematoxylin, dehydrated, and mounted in DePeX (BDH Ltd., Poole, England). Immunofluorescence was used for double labeling of epidermal ear sheets. Fixed tissues were incubated with the first mAb tissue culture supernatant overnight, washed, and incubated with GAM-FITC (15 μ g/ml) for 90 min. After washing, tissues were incubated with 30% mouse serum for 60 min, incubated with the second biotinylated IgG mAb (10 μ g/ml) for 4 h, washed, incubated with Texas red-conjugated streptavidin (10 μ g/ml) (Southern Biotechnology Associates, Inc.) for 90 min, washed, and mounted in Citifluor glycerol solution (Citifluor Ltd., London, England).

Cell Surface Radioiodination and Immunoprecipitation. 10⁷ density gradient-enriched veiled cells were surface labeled by an H₂O₂ lactoperoxidase-catalyzed radioiodination method (38). Labeled cells were solubilized in 500 μ l lysis buffer comprising 10 mM Tris-HCl, pH 7.5–8, 150 mM NaCl, 5 mM EDTA, 1% NP-40, 1 mM PMSF, and 5 mM iodoacetamide for 30 min at 4°C. Samples (2.5×10^6 cell equivalents) were centrifuged and the supernatants precleared for 30 min at 4°C on a rotating wheel with 100 μ l of a 10% suspension of Sepharose CL-4B beads (Pharmacia, Uppsala, Sweden), which had been covalently coupled to purified mAb IgG using cyanogen bromide (~ 10 mg purified mAb IgG/ml CL-4B beads) (39). Preclearing was repeated three times. Precleared samples were directly immunoprecipitated for 1 h at 4°C on a rotating wheel with 30 μ l of a 10% solution of Sepharose CL-4B beads covalently coupled to purified mAb IgG. Immunoprecipitated samples were washed in the following buffers: (a) 10 mM Tris-HCl, pH 8.0, containing 500 mM NaCl, 0.5% NP-40, and 0.05% SDS; (b) 10 mM Tris-HCl, pH 8.0, containing 150 mM NaCl, 0.5% NP-40, 0.5%

sodium deoxycholate, and 0.05% SDS; (c) 10 mM Tris-HCl, pH 8.0, containing 0.05% SDS. Samples and molecular weight markers (Rainbow™ protein molecular weight markers; Amersham, Bucks, England) were boiled in 15 μ l sample buffer for 5 min and run on 7.5% SDS-PAGE using a mini-gel apparatus (Bio-Rad Laboratories, Richmond, CA) (40). Gels were fixed, dried, and exposed to Hyperfilm™ (Amersham) at -70°C .

Western Blotting. Veiled cell-enriched lysates prepared as described for immunoprecipitation were run on 7.5% SDS-PAGE using a mini-gel apparatus (Bio-Rad Laboratories). Protein was transferred to nitrocellulose (Hybond™-C-extra; Amersham) using a mini trans-blot electrophoretic transfer apparatus (Bio-Rad Laboratories). Membranes were placed in PBS containing 5% dried nonfat milk powder for 24 h at 4°C . Ascites fluid containing the appropriate mAb was added to give a final concentration of 1–50 $\mu\text{g}/\text{ml}$, and the membranes were incubated for 2 h at 4°C with rocking. The membranes were washed three times in PBS/0.05% Tween 20 before addition of ^{125}I -RAM (sp act $\sim 1.5 \mu\text{Ci}/\mu\text{g}$ IgG at a dilution of 10^6 cpm/ml) in PBS/0.05% Tween 20/1% BSA. After incubation for 1 h at 4°C , the membranes were washed three times in PBS/0.05% Tween 20 and exposed to Hyperfilm™ at -70°C .

Results and Discussion

Production of the OX-62 mAb Out of a total of four fusions and screening $\sim 2,000$ wells, one hybridoma secreting a mouse anti-rat IgG1 mAb (OX-62) was selected on the basis of immunohistochemical staining of cells with dendritic cell morphology in tissue sections of lymphoid organs. In the current studies, $<10\%$ of the mAbs produced were against MHC class II antigens, although anti-MHC class II mAbs have been reported to comprise up to 50% of positive hybridomas in anti-dendritic cell fusions (16). A number of interesting mAbs against endothelial determinants were produced.

Expression of the OX-62 Antigen by Different Leukocyte Types. Fig. 1 shows FACScan® profiles of different isolated leukocyte types labeled with the OX-62 mAb. Positive profiles were only obtained with density gradient-enriched veiled cells from MLNX TDL (Fig. 1 C). Immunohistochemical staining of cytospin preparations of MLNX TDL and TDL confirmed that veiled cells were the only cell type labeled (Fig. 3, I and J). Thymocytes (Fig. 1 F), splenocytes (Fig. 1 G), and lymph node cells (Fig. 1 H), tissues known to have OX-62⁺ cells in low numbers by immunohistochemical staining of sections (Fig. 3, A, C, and E), gave staining with the OX-62 mAb at a level barely distinguishable from background on the FACScan®, indicating that the OX-62⁺ cells are normally present at too low a frequency to be clearly detectable by this method. Resident peritoneal exudate cells (Fig. 1 I), thioglycollate elicited peritoneal exudate cells (Fig. 1 J), LPS blasts (Fig. 1 K), and Con A blasts (Fig. 1 L), were OX-62⁻. The OX-62 mAb failed to label PBL and bone marrow cells when analyzed on a FACScan® (Fig. 1, D and E) and by immunohistochemical staining of cytospin preparations (data not shown).

Enrichment of Dendritic Cells. The infrequent distribution of dendritic cells makes isolation difficult. Dendritic cells can either be obtained in suspension in lymph or from lymphoid organs with or without enzyme digestion and adherence. Dendritic cells represent $\sim 1\%$ or less of these populations; therefore, further enrichment is dependent either on positive or negative selection using relevant mAbs and/or nonspecific separation using density gradients (41, 42).

The ability of the OX-62 mAb to enrich and deplete OX-62-labeled cells was assessed after magnetic sorting phenotypically by flow cytofluorography using a FACScan®, morphologically, and functionally using magnetically sorted cells

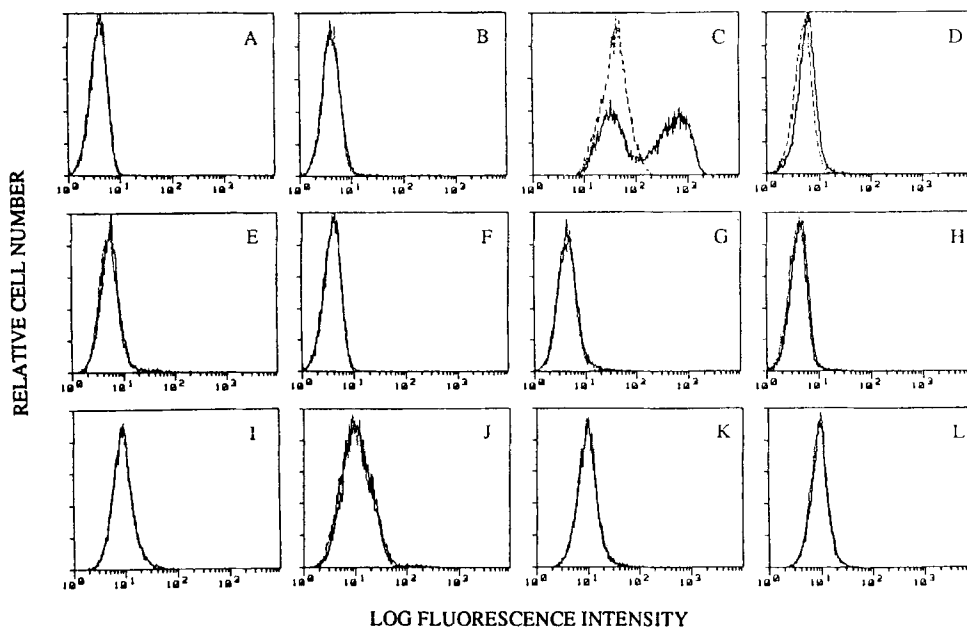


Figure 1. Binding of OX-62 mAb to different leukocyte types isolated from PVG rats. Cells were labeled with saturating levels of OX-62 mAb (—) and isotype-matched negative control OX-21 mAb (---) followed by a second incubation with RAM-FITC. Bound mAb was measured by flow cytofluorography. A, TDL; B, MLNX TDL; C, MLNX TDL gradient enriched for veiled cells ($\sim 50\%$ enrichment); D, PBL; E, bone marrow cells; F, thymocytes; G, splenocytes; H, lymph node cells; I, resident peritoneal exudate cells; J, thioglycollate elicited peritoneal exudate cells; K, LPS blasts; L, Con A blasts. Note all profiles are superimposed except for C and D.

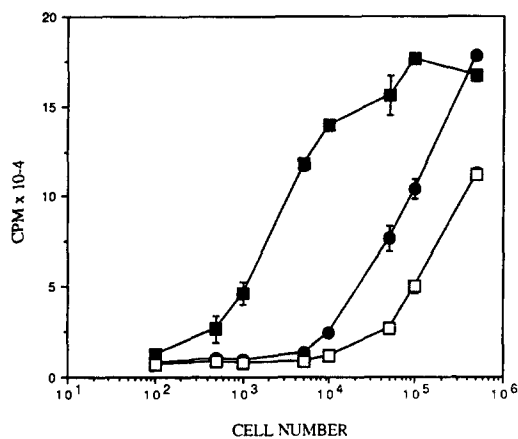


Figure 2. Comparison of OX-62⁺ cell-enriched and -depleted populations as stimulators in an MLR. 5×10^5 AO TDL responders depleted of OX-6-, OX-17-, OX-8-, and OX-12-labeled cells by magnetic sorting were stimulated with different numbers of unseparated PVG MLNX TDL (●), PVG MLNX TDL enriched for OX-62⁺ cells by magnetic sorting (■), and PVG MLNX TDL depleted of OX-62⁺ cells by magnetic sorting (□). Data are the mean and SD of quadruplicate cultures.

as stimulators in the primary allogeneic MLR. Magnetic sorting gave >75% enrichment of OX-62 mAb-labeled cells. The potency of the cell populations separated after labeling with the OX-62 mAb and used as stimulators in the primary allogeneic MLR is shown in Fig. 2. The OX-62-enriched cells were potent stimulators, with 1.22×10^3 cells per culture, providing the same stimulus as 15.5×10^3 unseparated cells. The depleted cells had 12% of the activity of the unseparated cells, indicating that the OX-62⁺ cells were the major stimulating cell in the MLR. It can be argued that almost all the stimulating activity is from OX-62⁺ cells, since the activity of the depleted cells is in accord with the level of OX-62⁺ cell contamination. Magnetic sorting of OX-62 mAb-labeled cells represents a useful method for enriching for veiled cells. To obtain purer populations of veiled cells (>90%) in high yields, magnetically sorted cells can be sorted by flow cytography using a FACS® (data not shown).

Effect of the OX-62 mAb on the Primary Allogeneic MLR. OX-62 IgG added at the start of culture in a concentration range from 1.25 ng/ml to 2.5 μg/ml had no effect on the MLR between CD4 responders from AO rats (i.e., OX-6, OX-17, OX-8, and OX-12 mAb-labeled and magnetically depleted TDL) and unseparated MLNX TDL stimulators from PVG rats (data not shown), indicating that the OX-62 antigen is not essential for T cell activation.

Distribution of the OX-62 Antigen in Lymphoid Organs. The distribution of the OX-62 antigen in lymphoid organs (Fig. 3) mostly coincided with previous reports of dendritic cell distribution based on microscopic and immunohistochemical studies (4, 6, 11, 13–16, 43–47). All cells labeled with the OX-62 mAb had a dendritic cell morphology. In the thymus, OX-62⁺ cells were present in the medulla forming a diffuse network, which was concentrated at the cortico-

medullary junction (Fig. 3 A). OX-62⁺ cells were also present in the lobular septa with occasional cells present in the cortex (Fig. 3 A), correlating with the large scattered cells observed in the cortex in bone marrow chimeras (43). In the spleen, OX-62⁺ cells were concentrated in the T-dependent areas, particularly around the region of the central arteriole but also throughout the red pulp (Fig. 3 C). The OX-62⁺ cells in the red pulp were rounded and more strongly stained compared with cells in the T-dependent areas where the borders were difficult to define. OX-62⁺ cells were present in the marginal zones and the peripheral white pulp infrequently (Fig. 3 C). In the cervical lymph node, OX-62⁺ cells were present in the subcapsular sinus, T-dependent areas of the cortex, and in the medulla, but were rare in the follicles (Fig. 3 E). In the Peyer's patch, OX-62⁺ cells were present in the interfollicular areas and in the epithelial dome regions, but were rare in the follicles (Fig. 3 C). Background staining with an isotype-matched mAb OX-21 was negligible (Fig. 3, B, D, F, and H). No difference in OX-62 staining was found between PVG, AO, DA, and Lewis rat strains, and OX-62⁺ cells were present in congenitally athymic PVG nude rats (PVG rnu/rnu) (data not shown), confirming previous results using anti-MHC class II mAbs (48).

Distribution of the OX-62 Antigen in Nonlymphoid Organs. OX-62⁺ cells with dendritic morphology that coincided with known MHC class II dendritic cell distribution (48, 49) were present in the lamina propria of the small intestine (Fig. 4, A and B), interstitium of the lung, portal triads of the liver, glomeruli of the kidney, islets of Langerhans of the pancreas, and epithelium of the choroid plexus (data not shown). Lack of OX-62⁺ cells in heart and skeletal muscle (data not shown) contrasts with previous studies using anti-MHC class II mAbs (48–50).

Unexpectedly, the OX-62 mAb revealed populations of OX-62⁺ MHC class II⁻ cells in the epithelium of the small intestine and in the epidermis of the skin. In the epithelium of the small intestine, only granular MHC class II staining has been reported (Fig. 4 B; and 47), but this staining was not associated with the OX-62⁺ intraepithelial cells (Fig. 4 A). In epidermal sheets, OX-62 mAb labeling primarily revealed cells with a marked dendritic morphology comprising the cell body and nonoverlapping dendritic processes (Fig. 4 C) in contrast to OX-6 mAb labeling, which primarily revealed cells with less prominent dendrites (Fig. 4 D). Double immunofluorescence showed that most if not all the OX-62⁺ and MHC class II⁺ populations were nonoverlapping (Fig. 4, E, F, and G). The OX-62⁺ MHC class II⁻ cells in the small intestine and the skin were CD3⁺ (data not shown) and probably represent γ/δ T cells (51–53). Overall, the results indicate that the OX-62 mAb may label some but not all dendritic cells and probably γ/δ T cells. Furthermore, the identification of nonoverlapping OX-62⁺ MHC class II⁻ and OX-62⁻ MHC class II⁺ populations in the skin with a similar distribution raises the question as to which cells migrate into the afferent lymphatics giving rise to the OX-62⁺ MHC class II⁺ veiled cells. Previous work has in-

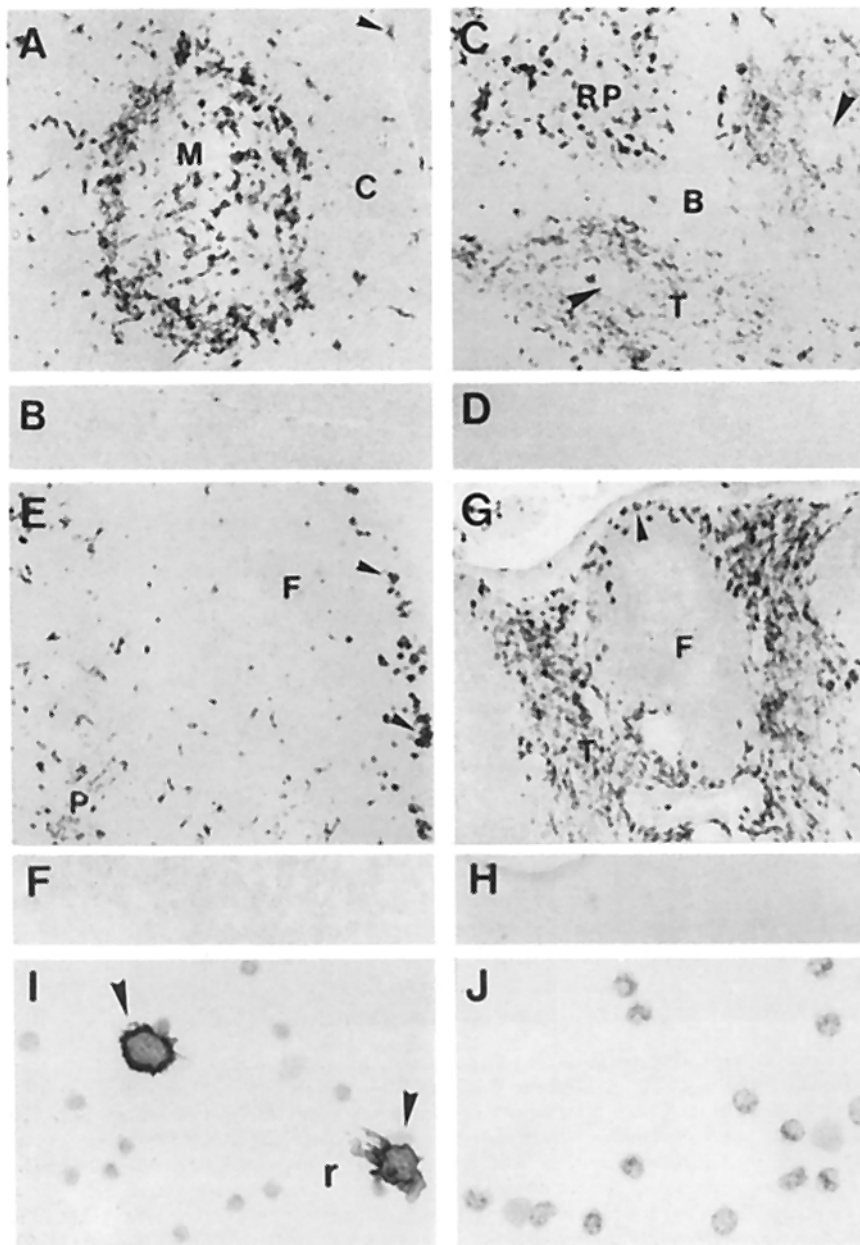


Figure 3. Binding of OX-62 mAb to PVG rat lymphoid tissues. Cryostat sections (5 μm) and cytopsin preparations labeled using the indirect immunoperoxidase method. *A*, thymus labeled with OX-62 mAb. Cells in the medulla (*M*) note concentration at the cortico-medullary junction, scattered cells in the cortex (*C*) and infrequent cells in the lobular septae (\blacktriangleright) labeled. *B*, thymus labeled with isotype-matched negative control OX-21 mAb. *C*, spleen labeled with OX-62 mAb. Cells in the T cell areas (*T*) of the white pulp surrounding the central arteriole (\blacktriangleright), infrequent cells in the B cell areas (*B*) of the white pulp, and cells in the red pulp (*RP*) labeled. *D*, spleen labeled with OX-21 mAb. *E*, cervical lymph node labeled with OX-62 mAb. Cells in the subcapsular sinus (\blacktriangleright) and paracortex (*P*) labeled, but few cells in the follicle (*F*) labeled. *F*, cervical lymph node labeled with OX-21 mAb. *G*, Peyer's patch labeled with OX-62 mAb. Cells in the interfollicular T-dependent areas (*T*) and dome epithelium (\blacktriangleright) labeled, but few cells in the follicle (*F*) labeled. *H*, Peyer's patch labeled with OX-21 mAb. *I*, PVG MLNX TDL labeled with OX-62 mAb. Note labeling of veiled cells with dendritic morphology (\blacktriangleright). *J*, PVG TDL labeled with OX-62 mAb. *A-H* $\times 60$, *I* and *J*, $\times 375$.

dedicated that MHC class II⁺ Langerhans cells (54) are the probable precursors (55–58).

Distribution of the OX-62 Antigen in Autoimmune Disease Models. The presence of cells with dendritic morphology in autoimmune diseases has been documented (59–61); therefore, the distribution of OX-62⁺ cells in cryostat sections of organs from rat models with autoimmune diabetes (62) and experimental allergic encephalomyelitis (63) was examined. Increased OX-62 mAb labeling of cells in the islets of Langerhans with leukocyte infiltrates in the pancreas of rats with autoimmune diabetes was found when compared with control nondiabetic rats (data not shown). Similarly, increased OX-62 mAb labeling of cells in lesions in the spinal cord of rats with experimental allergic encephalomyelitis was found,

in contrast to normal rats where OX-62⁺ cells were rare (data not shown). It has not been established whether the increased labeling represents upregulation of the OX-62 antigen or migration of OX-62⁺ cells into the lesions.

Molecular Characterization of the OX-62 Antigen. The OX-62 mAb immunoprecipitated four noncovalently associated bands from radioiodinated density gradient-enriched veiled cells under both nonreducing (Fig. 5, *A*, lane 1) and reducing (lane 2) conditions: a major band of ~ 150 kD, a minor band of ~ 120 kD that migrated faster under nonreducing conditions, and two lower bands of < 30 kD. The OX-62 mAb precleared all bands immunoprecipitated by the OX-62 mAb but some contaminants remained in the lowest apparent molecular mass band, which coincided with the dye

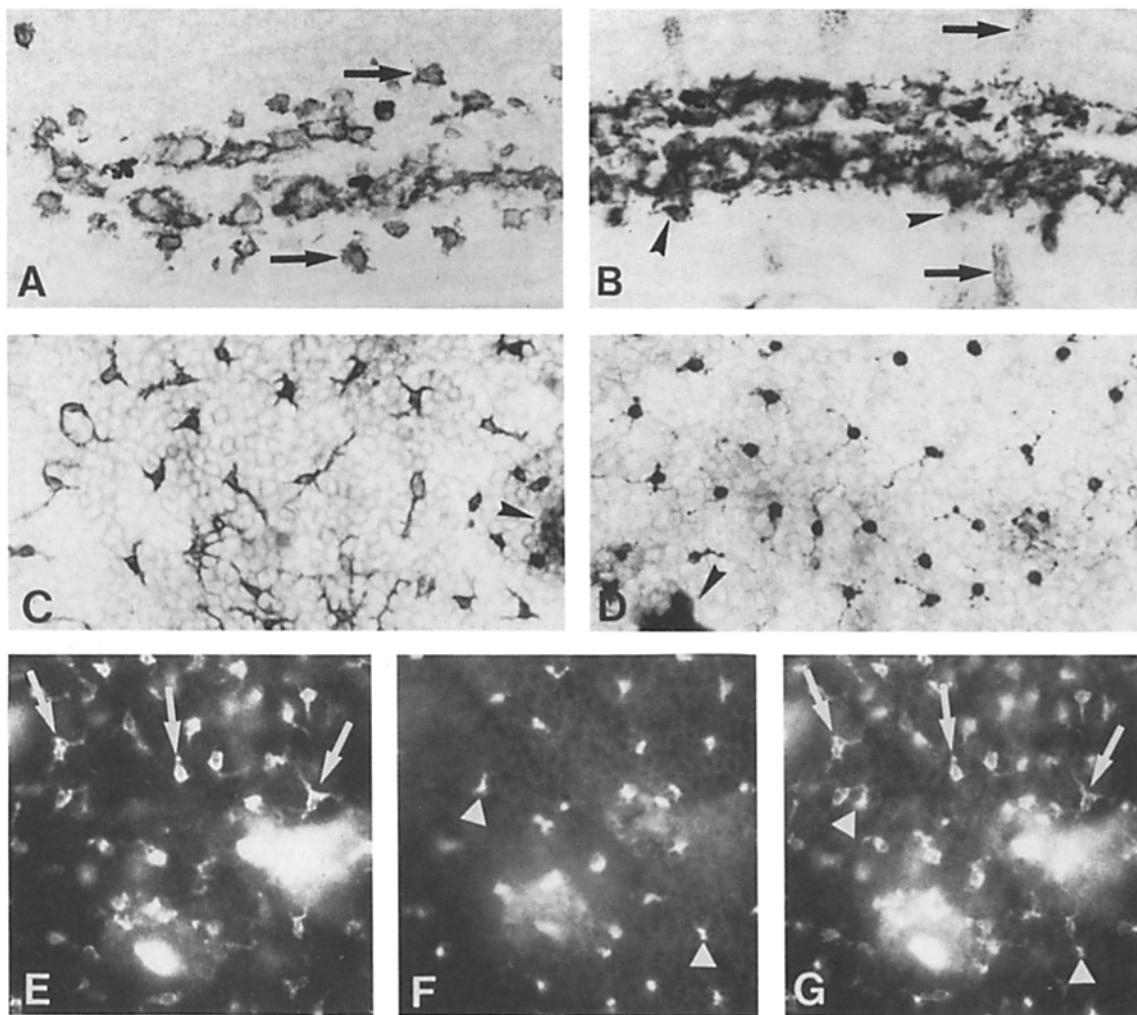


Figure 4. Labeling of OX-62⁺ MHC class II⁻ cells in the intraepithelial region of the small intestine and in epidermal ear sheets. PVG rat small intestine cryostat sections (5 μ m) (A and B) and epidermal ear sheets (C-G). A-D labeled using the indirect immunoperoxidase method; and E-G labeled using double immunofluorescence. A, OX-62 mAb. Cells in the lamina propria with dendritic morphology and smaller intraepithelial cells labeled (\rightarrow). B, OX-6 mAb. Cells in the lamina propria and cells with cytoplasmic processes extending into the epithelium labeled (\blacktriangleright). Note granular OX-6 mAb labeling of the epithelium (B, \rightarrow) compared with the OX-62 mAb intraepithelial cell labeling (A, \rightarrow). C, OX-62 mAb. Note labeling of dendritic processes. D, OX-6 mAb. Note rounded morphology and less prominent dendrites. Nonspecific staining represent hair follicles (C and D, \blacktriangleright). E, GAM-FITC detection of OX-62 mAb. F, streptavidin Texas red detection of OX-6 IgG biotin-conjugated mAb. G, combined GAM-FITC detection of the OX-62 mAb and streptavidin Texas red detection of OX-6 IgG biotin-conjugated mAb. Note nonoverlapping populations of OX-62⁺ and OX-6⁺ cells. Examples of nonoverlapping OX-62⁺ cells (\rightarrow) in E and G are missing in F. Examples of OX-6⁺ cells (\blacktriangle) in F and G are missing in E. Large fluorescent areas represent autofluorescence of hair follicles (E-G). A-D, $\times 250$; E and F, $\times 175$.

front (Fig. 5 A, lane 3). The 150-kD band was the only band detected by the OX-62 mAb on Western blots (Fig. 5 B, lane 1). The biochemical properties of the OX-62 antigen are characteristic of an integrin. Integrins consist of noncovalently associated α (120–210-kD) and β (95–220-kD) subunits (64). The strong 150-kD band present under nonreducing and reducing conditions is α subunit like and the weaker 120-kD band, which migrated faster under nonreducing conditions due to internal disulphide bonding (64), is β subunit like. The stronger 150-kD band would be predicted as the OX-62 mAb recognizes the 150-kD band, and the noncovalent association of α/β integrin subunits, which is weak under immunoprecipitation conditions, results in some coprecipita-

tion of α with β (65) and β with α (66). The β subunit is not β_1 , based on preclearing experiments with a cross-reactive antipeptide antibody (65) followed by immunoprecipitation (data not shown), and not β_2 , based on preclearing experiments with the OX-42 mAb (CD18/CD11b) followed by immunoprecipitation (data not shown). β_1 , β_2 , and β_7 (β_p) are present in lymphoid cells (64). The α subunit is not α^3 , α^5 , or α^6 , based on preclearing experiments with cross-reactive antipeptide antibodies (66) followed by immunoprecipitation (data not shown). The α subunits are grouped into those that have I domains and those that undergo posttranslational cleavage (α^3 , α^5 , and α^6) to give a cytoplasmic/transmembrane/extracellular fragment (25 kD)

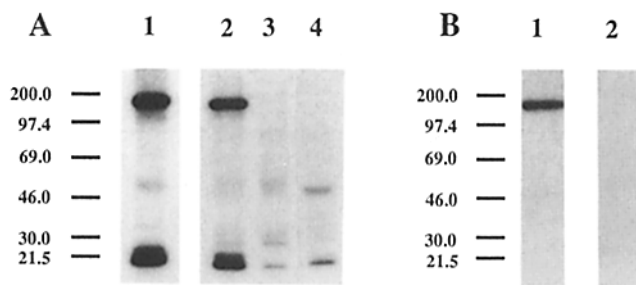


Figure 5. (A) Immunoprecipitation of the OX-62 antigen. A ^{125}I surface-labeled PVG veiled cell-enriched lysate was run on 7.5% SDS-PAGE before autoradiography. Samples were unreduced (lane 1) or reduced (lanes 2-4). (Lanes 1 and 2) OX-62 mAb immunoprecipitation after control SN3 mAb preclear. (Lane 3) OX-62 mAb immunoprecipitation after OX-62 mAb preclear. (Lane 4) Control SN3 mAb immunoprecipitation after control SN3 mAb preclear. (B) Western blotting of the OX-62 antigen. A PVG veiled cell-enriched lysate was run under reducing conditions on 7.5% SDS-PAGE and electroblotted to nitrocellulose. The nitrocellulose membranes were probed with (lane 1) OX-62 mAb, (lane 2) isotype-matched negative control OX-21 mAb, and ^{125}I -RAM as the second mAb before autoradiography. Numbers indicate the apparent molecular mass (kD) determined from marker proteins.

and a larger extracellular fragment (130-150 kD) (64). The two <30-kD bands (Fig. 5 A, lanes 1 and 2) may represent alternative splicing of the cytoplasmic tail similar to that described for α^3 and α^6 (67). The presence of cleaved fragments under nonreducing (Fig. 5 A, lane 1) and reducing (lane 2) conditions is not identical to previously described cleaved α subunits, which are disulphide bonded (64), with the exception of $\alpha^{\text{M290}}\beta_7$ (68, 69). The M290 mAb, which identifies β_7 as deduced from sequence homology (70, 71) associated with a novel α subunit, shows similar biochemical characteristics to the OX-62 antigen. It has been proposed that M290 (68-71), HML-1 (72, 73), ber-ACT8 (74), and RGL-1 (75), which labels rat veiled cells (data not shown), recognize an homologous antigen present on intraepithelial lymphocytes.

Concluding Statement. OX-62 mAb seems to be restricted to dendritic cells in lymphoid and nonlymphoid organs, and to CD3^+ cells with dendritic morphology, which are probably γ/δ T cells. The OX-62 antigen has the biochemical properties of an integrin. The mAb will be useful for cell purification, delineating lineage relationships among cells with dendritic morphology, and for molecular studies.

We thank Dr. E. Marcantonio for β_1 , α^3 , α^5 , and α^6 antipeptide antibodies, Dr. N. Cerf-Bensussan for the RGL-1 ascites, Mr. Les Haven for cutting cryostat sections, Ms. Debbie Fowell for providing diabetic pancreatic tissue, the Photographic Unit, and Prof. Alan Williams and Drs. Neil Barclay and Jasper Rees for helpful discussions and reading of the manuscript.

Address correspondence to M. Brenan, MRC Cellular Immunology Unit, Sir William Dunn School of Pathology, University of Oxford, Oxford OX1 3RE, England.

Received for publication 19 July 1991 and in revised form 20 February 1992.

References

- Metlay, J.P., E. Puré, and R.M. Steinman. 1989. Control of the immune response at the level of antigen-presenting cells: a comparison of the function of dendritic cells and B lymphocytes. *Adv. Immunol.* 47:45.
- Fossum, S. 1989. The life history of dendritic leukocytes (DL). *Curr. Top. Pathol.* 79:101.
- Steinman, R.M., and M.D. Witmer. 1978. Lymphoid dendritic cells are potent stimulators of the primary mixed leukocyte reaction in mice. *Proc. Natl. Acad. Sci. USA.* 75:5132.
- Veerman, A.J.P., and W. van Ewijk. 1975. White pulp compartments in the spleen of rats and mice. A light and electron microscopic study of lymphoid and non-lymphoid celltypes in T- and B- areas. *Cell Tissue Res.* 156:417.
- Witmer, M.D., and R.M. Steinman. 1984. The anatomy of peripheral lymphoid organs with emphasis on accessory cells: light-microscopic immunocytochemical studies of mouse spleen, lymph node, and Peyer's patch. *Am. J. Anat.* 170:465.
- Steinman, R.M., and Z.A. Cohn. 1973. Identification of a novel cell type in peripheral lymphoid organs of mice. 1. Morphology, quantitation, tissue distribution. *J. Exp. Med.* 137:1142.
- Nussenzweig, M.C., R.M. Steinman, J.C. Unkeless, M.D. Witmer, B. Gutchinov, and Z.A. Cohn. 1981. Studies of the cell surface of mouse dendritic cells and other leukocytes. *J. Exp. Med.* 154:168.
- Steinman, R.M., and Z.A. Cohn. 1974. Identification of a novel cell type in peripheral lymphoid organs of mice. 11. Functional properties in vitro. *J. Exp. Med.* 139:380.
- MacPherson, G.G. 1989. Lymphoid dendritic cells: their life history and roles in immune responses. *Res. Immunol.* 140:877.
- Nussenzweig, M.C., R.M. Steinman, M.D. Witmer, and B. Gutchinov. 1982. A monoclonal antibody specific for mouse dendritic cells. *Proc. Natl. Acad. Sci. USA.* 79:161.
- Kraal, G., M. Bree, M. Janse, and G. Bruin. 1986. Langerhans' cells, veiled cells, and interdigitating cells in the mouse recognized by a monoclonal antibody. *J. Exp. Med.* 163:981.
- Poulter, L.W., D.A. Campbell, C. Munro, and G. Janossy. 1986. Discrimination of human macrophages and dendritic cells by means of monoclonal antibodies. *Scand. J. Immunol.* 24:351.
- Bree, M., R.E. Mebius, and G. Kraal. 1987. Dendritic cells of the mouse recognized by two monoclonal antibodies. *Eur.*

- J. Immunol.* 17:1555.
14. Nagelkerken, L.M., B. Schutte, R.J.M. Stet, and P.J.C. van Breda Vriesman. 1987. Recognition of rat dendritic cells by a monoclonal antibody. *Scand. J. Immunol.* 26:347.
 15. Maruyama, T., S. Tanaka, B. Bozoky, F. Kobayashi, and H. Uda. 1989. New monoclonal antibody that specifically recognizes murine interdigitating and Langerhans cells. *Lab. Invest.* 61:98.
 16. Metlay, J.P., M.D. Witmer-Pack, R. Agger, M.T. Crowley, D. Lawless, and R.M. Steinman. 1990. The distinct leukocyte integrins of mouse spleen dendritic cells as identified with new hamster monoclonal antibodies. *J. Exp. Med.* 171:1753.
 17. Holowachuk, E.W., J.K. Stoltenberg, W.E. Bowers, and E.M. Goodell. 1991. Mouse α rat dendritic cell-specific monoclonal antibodies: characterization of antigens. 75th Annual Meeting, Atlanta, Georgia. *FASEB (Fed. Am. Soc. Exp. Biol.) J.* 3634 (Abstr.)
 18. Cohen, D.A., and A.M. Kaplan. 1981. Adherent Ia⁺ murine tumor lines with characteristics of dendritic cells. 1. Morphology, surface phenotype, and induction of syngeneic mixed lymphocyte reactions. *J. Exp. Med.* 154:1881.
 19. Clayberger, C., R.H. DeKruyff, R. Fay, and H. Cantor. 1985. Identification of a unique B-cell-stimulating factor produced by a cloned dendritic cell. *Proc. Natl. Acad. Sci. USA.* 82:183.
 20. Breel, M., J. Laman, and G. Kraal. 1988. Murine hybrid cell lines expressing the NLDC-145 dendritic cell determinant. *Immunobiology.* 178:167.
 21. Ford, W.L., and S.V. Hunt. 1973. The preparation and labeling of lymphocytes. In *Handbook of Experimental Immunology*, 2nd ed. D.M. Weir, editor. Blackwell Scientific Publications, Oxford, England. 23.1-23.27.
 22. de St. Groth, S.F., and D. Scheidegger. 1980. Production of monoclonal antibodies: strategy and tactics. *J. Immunol. Methods.* 35:1.
 23. Galfrè, G., and C. Milstein. 1981. Preparation of monoclonal antibodies: strategies and procedures. *Methods Enzymol.* 73:3.
 24. Williams, A.F., A.G.D. Tse, and J. Gagnon. 1988. Squid glycoproteins with structural similarities to Thy-1 and Ly-6 antigens. *Immunogenetics.* 27:265.
 25. McMaster, W.R., and A.F. Williams. 1979. Identification of Ia glycoproteins in rat thymus and purification from rat spleen. *Eur. J. Immunol.* 9:426.
 26. Brideau, R.J., P.B. Carter, W.R. McMaster, D.W. Mason, and A.F. Williams. 1980. Two subsets of rat T lymphocytes defined with monoclonal antibodies. *Eur. J. Immunol.* 10:609.
 27. Hunt, S.V., and M.H. Fowler. 1981. A repopulation assay for B and T lymphocyte stem cells employing radiation chimaeras. *Cell Tissue Kinet.* 14:445.
 28. Fukumoto, T., W.R. McMaster, and A.F. Williams. 1982. Mouse monoclonal antibodies against rat major histocompatibility antigens. Two Ia antigens and expression of Ia and class I antigens in rat thymus. *Eur. J. Immunol.* 12:237.
 29. Hsiung, L., A.N. Barclay, M.R. Brandon, E. Sim, and R.R. Porter. 1982. Purification of human C3b inactivator by monoclonal-antibody affinity chromatography. *Biochem. J.* 203:293.
 30. Robinson, A.P., T.M. White, and D.W. Mason. 1986. Macrophage heterogeneity in the rat as delineated by two monoclonal antibodies MRC OX-41 and MRC OX-42, the latter recognizing complement receptor type 3. *Immunology.* 57:239.
 31. Mason, D.W., and A.F. Williams. 1980. The kinetics of antibody binding to membrane antigens in solution and at the cell surface. *Biochem. J.* 187:1.
 32. Mason, D.W., W.J. Penhale, and J.D. Sedgwick. 1987. Preparation of lymphocyte subpopulations. In *Lymphocytes a practical approach*. G.G.B. Klaus, editor. IRL Press, Oxford, England. 35-54.
 33. Jensenius, J.C., and A.F. Williams. 1974. The binding of anti-immunoglobulin antibodies to rat thymocytes and thoracic duct lymphocytes. *Eur. J. Immunol.* 4:91.
 34. Sorting cells with MACS. Instructions for use. 1990. Miltenyi Biotec, Gladbach, West Germany 1-15.
 35. Miltenyi, S., W. Müller, W. Weichel, and A. Radbruch. 1990. High gradient magnetic cell separation with MACS. *Cytometry.* 11:231.
 36. Bergstresser, P.R., and D.V. Juarez. 1984. Detection by immunocytochemical techniques of cell surface markers on epidermal Langerhans cells. *Methods Enzymol.* 108:683.
 37. Barclay, A.N. 1981. The localization of populations of lymphocytes defined by monoclonal antibodies in rat lymphoid tissues. *Immunology.* 42:593.
 38. Goding, J.W. 1986. Membrane and secretory immunoglobulins: structure, biosynthesis, and assembly. In *Handbook of Experimental Immunology* 4th ed. vol. 1. D.M. Weir, editor; L.A. Herzenberg, C. Blackwell, and Leonore A. Herzenberg, co-editors. Blackwell Scientific Publications, Oxford, England. 20.1-20.33.
 39. Porath, J. 1974. General methods and coupling procedures. *Methods Enzymol.* 73:13.
 40. Laemmli, U.K. 1970. Cleavage of structural proteins during the assembly of the head of bacteriophage T4. *Nature (Lond.)* 227:680.
 41. Klinkert, W.E.F. 1990. Lymphoid dendritic accessory cells of the rat. *Immunol. Rev.* 117:103.
 42. Crowley, M.T., K. Inaba, M.D. Witmer-Pack, S. Gezelter, and R.M. Steinman. 1990. Use of the fluorescence activated cell sorter to enrich dendritic cells from mouse spleen. *J. Immunol. Methods.* 133:55.
 43. Barclay, A.N., and G. Mayrhofer. 1981. Bone marrow origin of Ia-positive cells in the medulla of rat thymus. *J. Exp. Med.* 153:1666.
 44. Duijvestijn, A.M., and E.C.M. Hoefsmit. 1981. Ultrastructure of the rat thymus: the micro-environment of T-lymphocyte maturation. *Cell Tissue Res.* 218:279.
 45. van Ewijk, W. 1984. Immunohistology of lymphoid and non-lymphoid cells in the thymus in relation to T lymphocyte differentiation. *Am. J. Anat.* 170:311.
 46. Fossum, S. 1980. The architecture of rat lymph nodes. II. Lymph node compartments. *Scand. J. Immunol.* 12:411.
 47. Mayrhofer, G., C.W. Pugh, and A.N. Barclay. 1983. The distribution, ontogeny and origin in the rat of Ia-positive cells with dendritic morphology and of Ia antigen in epithelia, with special reference to the intestine. *Eur. J. Immunol.* 13:112.
 48. Hart, D.N.J., and J.W. Fabre. 1981. Demonstration and characterization of Ia-positive dendritic cells in the interstitial connective tissues of rat heart and other tissues, but not brain. *J. Exp. Med.* 153:347.
 49. Steiniger, B., J. Klemmner, and K. Wonigeit. 1984. Phenotype and histological distribution of interstitial dendritic cells in the rat pancreas, liver, heart, and kidney. *Transplantation (Baltimore).* 38:169.
 50. Spencer, S.C., and J.W. Fabre. 1990. Characterization of the tissue macrophage and the interstitial dendritic cell as distinct leukocytes normally resident in the connective tissue of rat heart. *J. Exp. Med.* 171:1841.
 51. Tschachler, E., G. Schuler, J. Hutterer, H. Leibl, K. Wolff, and G. Stingl. 1983. Expression of Thy-1 antigen by murine

- epidermal cells. *J. Invest. Dermatol.* 81:282.
52. Bergstresser, P.R., R.E. Tigelaar, J.H. Dees, and J.W. Streilein. 1983. Thy-1 antigen-bearing dendritic cells populate murine epidermis. *J. Invest. Dermatol.* 81:286.
 53. Lefrançois, L. 1991. Intraepithelial lymphocytes of the intestinal mucosa: curiouser and curiouser. *Semin. Immunol.* 3:99.
 54. Rowden, G., M.G. Lewis, and A.K. Sullivan. 1977. Ia antigen expression on human epidermal Langerhans cells. *Nature (Lond.)* 268:247.
 55. Silberberg-Sinakin, I., G.J. Thorbecke, R.L. Baer, S.A. Rosenthal, and V. Berezowsky. 1976. Antigen-bearing Langerhans cells in skin, dermal lymphatics and in lymph nodes. *Cell. Immunol.* 25:137.
 56. Schuler, G., and R.M. Steinman. 1985. Murine epidermal Langerhans cells mature into potent immunostimulatory dendritic cells in vitro. *J. Exp. Med.* 161:526.
 57. Cumberbatch, M., and I. Kimber. 1990. Phenotypic characteristics of antigen-bearing cells in the draining lymph nodes of contact sensitized mice. *Immunology.* 71:404.
 58. Larsen, C.P., R.M. Steinman, M. Witmer-Pack, D.F. Hankins, P.J. Morris, and J.M. Austyn. 1990. Migration and maturation of Langerhans cells in skin transplants and explants. *J. Exp. Med.* 172:1483.
 59. Knight, S.C., J. Mertin, A. Stackpoole, and J. Clark. 1983. Induction of immune responses *in vivo* with small numbers of veiled (dendritic) cells. *Proc. Natl. Acad. Sci. USA.* 80:6032.
 60. Born, W.K., R.L. O'Brien, and R.L. Modlin. 1991. Antigen specificity of $\gamma\delta$ T lymphocytes. *FASEB (Fed. Am. Soc. Exp. Biol.) J.* 5:2699.
 61. King, P.D., and D.R. Katz. 1990. Mechanisms of dendritic cell function. *Immunol. Today.* 11:206.
 62. Penhale, W.J., P.A. Stumbles, C.R. Huxtable, R.J. Sutherland, and D.W. Pethick. 1990. Induction of diabetes in PVG/c strain rats by manipulation of the immune system. *Autoimmunity.* 7:169.
 63. Raine, C.S. 1984. Biology of disease. Analysis of autoimmune demyelination: its impact upon multiple sclerosis. *Lab. Invest.* 50:608.
 64. Hemler, M.E. 1990. VLA proteins in the integrin family: structures, functions, and their role on leukocytes. *Annu. Rev. Immunol.* 8:365.
 65. Marcantonio, E.E., and R.O. Hynes. 1988. Antibodies to the conserved cytoplasmic domain of the integrin β_1 subunit react with proteins in vertebrates, invertebrates, and fungi. *J. Cell Biol.* 106:1765.
 66. Hynes, R.O., E.E. Marcantonio, M.A. Stepp, L.A. Urry, and G.H. Yee. 1989. Integrin heterodimer and receptor complexity in avian and mammalian cells. *J. Cell Biol.* 109:409.
 67. Tamura, R.N., H.M. Cooper, G. Collo, and V. Quaranta. 1991. Cell type-specific integrin variants with alternative α chain cytoplasmic domains. *Proc. Natl. Acad. Sci. USA.* 88:10183.
 68. Kilshaw, P.J., and K.C. Baker. 1988. A unique surface antigen on intraepithelial lymphocytes in the mouse. *Immunol. Lett.* 18:149.
 69. Kilshaw, P.J., and S.J. Murant. 1990. A new surface antigen on intraepithelial lymphocytes in the intestine. *Eur. J. Immunol.* 20:2201.
 70. Kilshaw, P.J., and S.J. Murant. 1991. Expression and regulation of β_7 (β_p) integrins on mouse lymphocytes: relevance to the mucosal immune system. *Eur. J. Immunol.* 21:2591.
 71. Yuan, Q., W. Jiang, D. Hollander, E. Leung, J.D. Watson, and G.W. Krissansen. 1991. Identity between the novel integrin β_7 subunit and an antigen found highly expressed on intraepithelial lymphocytes in the small intestine. *Biochem. Biophys. Res. Commun.* 176:1443.
 72. Cerf-Bensussan, N., A. Jarry, N. Brousse, B. Lisowska-Groszpiere, D. Guy-Grand, and C. Griscelli. 1987. A monoclonal antibody (HML-1) defining a novel membrane molecule present on human intestinal lymphocytes. *Eur. J. Immunol.* 17:1279.
 73. Cerf-Bensussan, N., B. Bègue, J. Gagnon, and T. Meo. 1992. The human intraepithelial lymphocyte marker HML-1 is an integrin consisting of a β_7 subunit associated with a distinctive α chain. *Eur. J. Immunol.* 22:273.
 74. Kruschwitz, M., G. Fritzsche, R. Schwarting, K. Micklem, D.Y. Mason, B. Falini, and H. Stein. 1991. Ber-ACT8: new monoclonal antibody to the mucosa lymphocyte antigen. *J. Clin. Pathol.* 44:636.
 75. Cerf-Bensussan, N., D. Guy-Grand, B. Lisowska-Groszpiere, C. Griscelli, and A.K. Bhan. 1986. A monoclonal antibody specific for rat intestinal lymphocytes. *J. Immunol.* 136:76.